Defect-Induced Oxidation of Graphite

Seung Mi Lee,[1] Young Hee Lee,[1,*] Yong Gyoo Hwang,[2] J. R. Hahn,[3] and H. Kang[3]
[1]*Department of Semiconductor Science and Technology, Department of Physics and Semiconductor Physics Research Center, Jeonbuk National University, Jeonju 561-756, South Korea*
[2]*Department of Physics, Wonkwang University, Iksan, Jeonbuk 570-749, South Korea*
[3]*Department of Chemistry, Pohang University of Science and Technology, Pohang, Gyeong-buk, 790-784, South Korea*
(Received 10 September 1998)

Atomic vacancies with controlled depth and size are generated on a graphite surface by low-energy ion bombardment. The reactivity of vacancies towards an oxygen molecule is investigated by using scanning tunneling microscopy (STM) and density functional theory. An oxygen molecule (i) exothermally dissociates and then chemisorbs at the top sites and/or the bridge sites of a vacancy, or (ii) forms a precursor state of molecular oxygen at a bridge site. Reaction pathways for oxidative etching are proposed to interpret serpentine and circular etching patterns observed by STM. [S0031-9007(98)08058-2]

PACS numbers: 82.30.–b, 68.45.Da, 81.65.Mq

Understanding of the oxidative etching process of a basal plane of graphite is both scientifically and technologically important. This subject is related to carbon combustion, coal gasification, reactions at nuclear reactor walls, and reentry shields of space crafts. In early studies, the etch-decoration transmission electron microscopy technique was very successful in examining the kinetics of oxidative etching processes, by measuring the lateral growth rate of etch pits produced by the reaction of O_2 molecules with natural defects on graphite [1–3]. These studies suggested that O_2 molecules first react with carbon atoms at defect sites to form adsorbed products, which eventually desorb to the gas phase.

Two independent reaction mechanisms have been proposed for the growth of etch pits [3]: (i) reaction from direct collisions of O_2 molecules on reactive carbon sites [Eley-Rideal (ER) mechanism]; (ii) the surface migration mechanism, i.e., reaction with the migrating oxygen molecules that are first adsorbed on nonreactive sites [Langmuir-Hinshelwood mechanism]. More recently scanning tunneling microscopy (STM) measurements showed that only monolayer etching occurred from natural defects [4–6]. Pits were uniform in size, indicating that the growth was simultaneously initiated at surface defects [6]. Various etching patterns have also been seen under catalytic reaction conditions [4]. Monolayer etching produced mainly CO gas, whereas the production ratio of CO_2 to CO gas increased in highly damaged graphite surfaces [7–9]. Despite these efforts, understanding mechanistic details of CO and CO_2 gas formation during the etching process is a long standing problem. Such difficulty arises mainly from two factors: (i) oxidation started from defect sites that were poorly characterized in the previous works; (ii) an atomistic model for the reaction of O_2 molecules with graphite was absent, which is an essential ingredient for atomic-level interpretation of the kinetics.

In this paper, we have carried out a systematic study for the reaction of O_2 at a vacancy of a graphite surface using the STM measurements and density functional (DF) calculations. Atomic defects are intentionally generated on a graphite surface with controlled depth and size by low-energy ion bombardment. Etching behaviors from these defects by the reaction of O_2 molecules are investigated with STM measurement. The etching speed and pattern vary substantially depending on whether they start from a monolayer or a multilayer defect. This observation strongly indicates that several types of initial adsorption states for an oxygen molecule are involved in the etching process. We identify key intermediates in the oxidation process using the DF calculations. Our calculations show that an O_2 molecule dissociatively adsorbs at a vacancy site of graphite exothermally without an energy barrier. An O_2 molecule dissociates at a divacancy to bind O atoms at either two bridge sites or two top sites. We also find a geometry in which an O_2 molecule does not dissociate but instead forms an O_2^* molecular precursor state. Based on our calculations, we propose reaction pathways of oxidative etching processes which can produce CO and CO_2 gases and the different etching patterns.

Atomic vacancies are generated on a highly oriented pyrolytic graphite surface by low-energy Ar^+ ion bombardments. By tuning the ion impact energy in the region of threshold energy of the defect formation (40–200 eV), we are able to control the size (mono-, di-, and triatomic vacancies) and the depth (first, second, and third graphite layers) of vacancies [10,11]. The defected surface is etched with O_2 molecules by heating a sample to 500–600 °C in dry air. The O_2 reaction transforms atomic vacancies into large-size pits. Figure 1 exemplifies the evolution of vacancies to etch pits, showing STM topographic images of a surface at various stages of oxidative etching. In the STM image of Fig. 1(a), vacancies generated by 100 eV Ar^+ impacts appear as small bright spots. The bright STM image of defect is due to the increase of the local charge density near the Fermi level [10]. At an initial stage of oxidative etching [Fig. 1(b)], etch pits

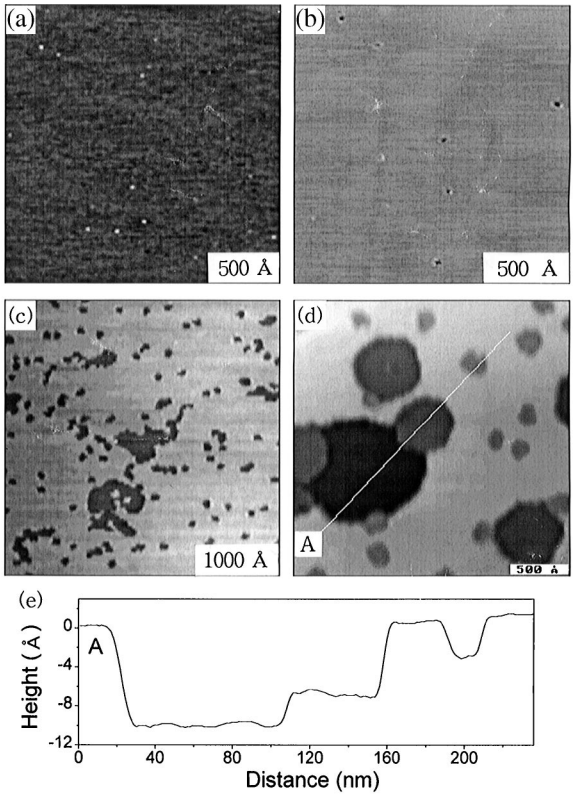

FIG. 1. STM images of etched structures initiated by atomic defects produced by low-energy ion bombardments. (a) An image of defects produced by 100 eV Ar^+ collision. The hillocks represent defect structures. An early stage of O_2 etching after heating the surface (a) at 560 °C for (b) 8 min and (c) 12 min, respectively. Certain pits in (c) exhibit anisotropic etching patterns. (d) The image showing mono-, double-, and triple-layer etch pits. Initial defects are produced by 300 eV Ar^+ impacts. (e) The cross-sectional cut of the image (d) along the line *A*.

appear as a pinhole at the center of a bright spot as its size is less than a few nm in diameter. Further oxidation increases the etched area [Fig. 1(c)]. Most of the etch pits have nearly circular shapes. Etching of monolayer pits occurs sometimes in serpentine patterns. Multilayer vacancies are generated by higher energy ion collisions. Etch pits resulting from multilayer vacancies are shown in Fig. 1(d). The cross-sectional cut of STM topography is presented in Fig. 1(e) in order to label the depth of pits. Vertical etching does not occur at the employed temperatures [4]. Thus the multilayer pits originate solely from multilayer defects artificially created by ion impact. Multilayer pits grow faster than monolayer pits. This allows us to distinguish mono-, double-, and triple-layer pits in STM images from their diameter, even without measuring depth. The ratio among average diameters of mono-, double-, and triple-layer pits is 1.0:3.2:7.0 at a given etching temperature and time. The detail for STM measurements can be found elsewhere [11].

We also perform DF total energy calculations based on local density approximation (LDA) and generalized gradient approximation (GGA), as implemented in the DMOL3 code [12]. The exchange-correlation energy in LDA is parametrized by Perdew and Wang's scheme [13], and Becke's corrected exchange functional [14] is adopted in GGA calculations. All-electron Kohn-Sham wave functions are expanded in a local atomic orbital basis. All orbitals including core electrons, are taken into account throughout the calculations. In the double-numerical basis set [12], C-2*s* and C-2*p* orbitals are represented by two basis functions each, and a 3*d*-type wave function on carbon and oxygen atoms is used to describe polarization. The convergence criterion for the structure optimization is that all forces be ≤ 0.002 a.u. Structure optimization is done by the LDA scheme only. The GGA calculations are done with structures optimized by LDA whenever necessary.

We model a graphite surface by introducing a supercell of a (4×4) graphitic sheet with periodic boundary conditions applied along the planar directions to simulate an infinite graphitic layer [15]. The distance between layers is 3.4 Å and we neglect van der Waals interaction between layers since this interaction is much weaker than the covalent one. The surface is simulated by periodically repeated slabs of a graphitic monolayer parallel to the surface direction with a vacuum region of 7 Å.

A carbon atom is removed to create a vacancy and relaxed by LDA calculation [15]. Carbon atoms with dangling bonds form short bonds (1.38 Å) with their adjacent carbon atoms, compared to an ideal bond of graphite (1.42 Å), as shown in Fig. 2(a). We now add an O_2 molecule to this vacancy. We tried various initial configurations, for instance, an O_2 molecule is placed within the atomic plane as shown in Fig. 2(b), and an O_2 molecule is located laterally above the plane as shown in Fig. 2(c). In any case, an O_2 molecule exothermally dissociates and chemisorbs on the top and bridge sites, as shown in Fig. 2(d). The exothermic energy for creating two oxygen atoms at the top and bridge sites from an O_2 molecule is 9.7 (8.9) eV from LDA (GGA) calculations. When an O_2 molecule approaches dangling bonds at a vacancy, charges are transferred from carbon atoms to the oxygen molecule due to the larger electronegativity of oxygen atoms. The resulting intramolecular Coulomb repulsion breaks the O-O bond exothermally without an activation barrier. This interaction keeps the oxygen atoms apart, placing them at the opposite sides of the plane as shown in Fig. 2(d) [16].

We calculate the adsorption of an O_2 molecule at a divacancy. One of the backbonds is contracted to 1.38 Å. When an O_2 molecule approaches the middle of two dangling bonds at a divacancy with the O_2 molecular axis parallel to the atomic plane, it exothermally dissociates and chemisorbs at two top sites as shown in Fig. 3(b). The exothermic energy of two C-O bonds at the top sites from an O_2 molecule is 12.0 (10.4) eV from LDA (GGA) calculations (strictly speaking, this includes the relaxation energy of adjacent carbon atoms). The C-O bond length is 1.22 Å, almost the same as 1.23 Å of a C-O bond of

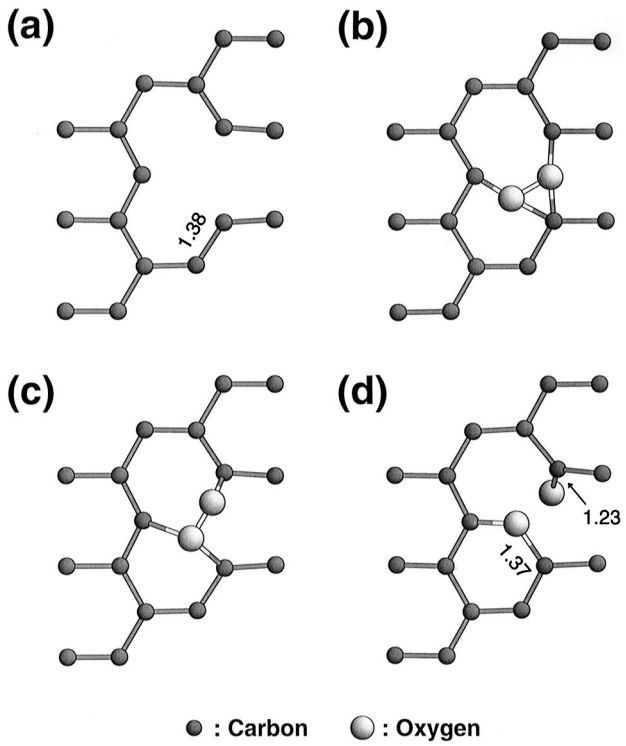

FIG. 2. Fully relaxed local geometries in a ball and stick form for (a) a single vacancy, (b) the initial position of an O_2 molecule squeezed in the vacancy, (c) a different initial position of an O_2 molecule located above the plane, and (d) an optimized O_2 adsorption at the top and bridge sites, where the oxygen atom at the top site is located below the plane. Bond lengths are in units of Å.

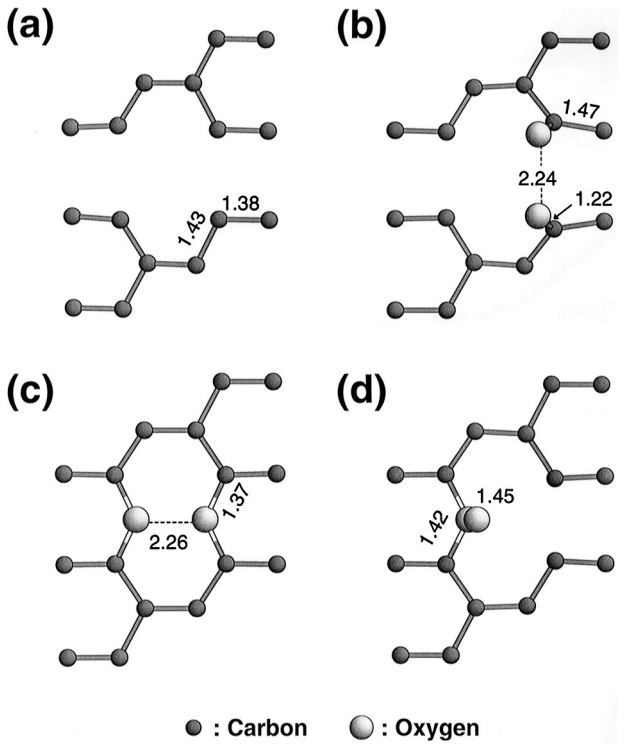

FIG. 3. Fully relaxed local geometries in a ball and stick form for (a) a divacancy, (b) an optimized O_2 adsorption at two top sites, where oxygen atoms are located above the graphitic plane, (c) an optimized O_2 adsorption at two bridge sites, and (d) an O_2 molecule located at a single bridge site. Bond lengths are in units of Å.

the top site at a single vacancy, but a little longer than that of a CO molecule (1.13 Å). The O-O distance is 2.24 Å, with oxygen atoms repelling each other. The situation is different when an O_2 molecule adsorbs at the center of a divacancy parallel to the missing carbon dimer. An O_2 molecule now saturates all of the dangling bonds, by taking two bridge sites as shown in Fig. 3(c). The exothermic energy of two C-O bonds at the bridge site is 16.6 (14.2) eV from LDA (GGA) calculations. The C-O bond length is 1.37 Å, the same as that at the bridge site of a single vacancy. The O-O distance is 2.26 Å, similar to that at two top sites.

We find another stable configuration, an O_2^* molecular precursor state, as shown in Fig. 3(d). This occurs when an O_2 molecule approaches the bridge site perpendicular to the atomic plane. In this case, the O-O bond is kept with the binding energy of -0.95 eV (LDA) with a bond length of 1.45 Å, longer than that of an O_2 molecule (1.21 Å). The oxygen atom on top of the C-O bond will be easily desorbed at typical etching temperatures and can participate in the oxidation at other active sites. We note that this type of an O_2^* precursor state does not exist at the top sites. An oxygen atom is exothermally released at one top site and adsorbed to another top site nearby.

We now describe the oxidative etching process that forms the CO and CO_2 gases based on our calculations. This is drawn in Fig. 4 for a divacancy. An O_2 molecule will dissociate and be adsorbed at either two top sites or two bridge sites. The adsorption at two top sites and two bridge sites will gain the energy of -5.5 (-4.9) and -10.1 (-8.6) eV, respectively. Since the C-O bond is more stable at the bridge site than at the top site, C-O at the top site is more liable to be etched away to form CO gas at typical temperatures. Note that CO backbonds at the top site are already stretched upward and form two single bonds with a bond length of 1.47 Å, as shown in Fig. 3(b), suggesting that more serious bond stretching of carbon backbonds is involved at the top sites. During this reaction, the free energy is increased by 2.6 (1.6) eV, but is still lower than that of the initial state by 2.9 (3.3) eV. Thus the reaction of exothermal dissociation of O_2 molecules and the activated CO desorption from the top sites is the primary etching process, following ER mechanism. Unlike at the top sites, the C-O bond at the bridge site is strongly bound and is very unlikely to be etched away under normal circumstances. Yet, oxygen atoms at bridge sites as well as at top sites can be etched away to form CO_2 gas by the assistance of an energetic CO molecule formed at other sites. The free energy is increased in this process by 0.9 (0.6) eV but is still much lower than that of the initial stage of an O_2 molecule. Thus CO_2 can be formed only by a secondary etching process involving energetic the CO gas. This explains why the CO production rate is

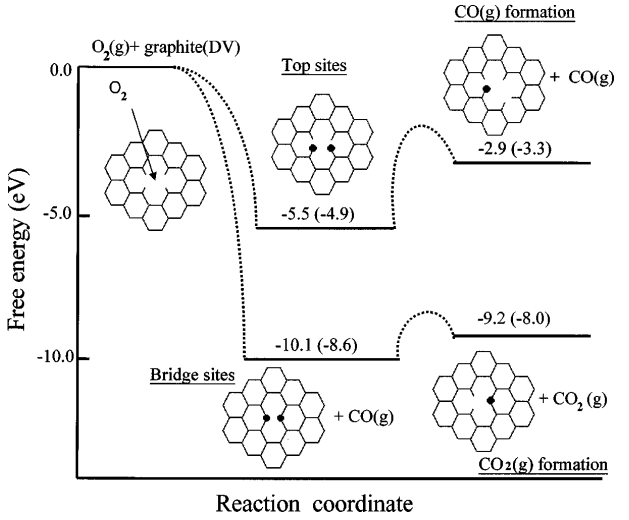

FIG. 4. The reaction pathways upon the O_2 adsorption and desorption processes to form CO and CO_2 gases via the top and bridge sites at a divacancy.

larger than the CO_2 production rate under normal oxidative etching conditions of a graphite [8,17]. We note that, when the CO backbond at a bridge site exceeds the bond length of 1.6 Å, CO_2 is immediately formed. Oxygen atoms, which can easily be released from O_2^* precursor states, can migrate on the surface and be adsorbed on the top and bridge sites at vacancies without an activation barrier.

The reaction pathways mentioned in the previous paragraph provide a comprehensive picture for different etching patterns observed by STM. In monolayer etching, with a continuous supply of O_2 molecules to vacancies, both top and bridge sites can be formed. The CO at the top site can be etched away by a thermally activated process, while CO at the bridge site is unlikely to be etched away due to the stronger binding energy. Once a CO at the top site is desorbed, two dangling bonds are newly created, again favoring the formation of either two top sites or an O_2^* precursor state. If two top sites are formed, etching will further continue in the same direction. If an O_2^* precursor state is formed, etching will not proceed to that direction. Still, etching may be continued in other directions where reactive top sites exist. This leads to an anisotropic etching, i.e., a serpentine etching pattern, as shown in Fig. 1(c). In the multilayer etching, an O_2 molecule can be supplied to the vacancy in the sublayer to form again the top and bridge sites [16]. The CO at the top site can be desorbed, similar to a single layer etching. However, CO gas desorbed in the sublayer migrates out and is able to collide with an oxygen atom in the top layer. This allows one to remove an oxygen atom not only at the top sites but also at the bridge sites, by forming CO_2 gas. This energetic CO species on the sublayer allow more efficient production of CO_2 gas in multilayer etching, as was observed in thermal desorption spectrometry [9]. Since this occurs randomly, anisotropic etching is relatively suppressed and a circular etching pattern should appear in the multilayer etching.

In summary, the reaction of an O_2 molecule with vacancies in a graphite surface has been investigated using STM and DF calculations. The O_2 molecules exothermally dissociate and adsorb at the dangling bonds of a vacancy. We have identified several types of adsorption sites: top site, bridge site, and O_2^* molecular precursor state at the bridge site. Reaction pathways to produce CO and CO_2 gases by activation processes have been described based on calculations. This paper presents the first experimental demonstration for the oxidative etching behavior of depth-differentiated atomic defects. This observation, aided by DF calculations identifying the key intermediate states, provides adequate atomistic interpretation of the graphite etching process.

We acknowledge the financial support by the KOSEF through the SPRC at JNU, and the CRI project from STEPI.

*Author to whom correspondence should be addressed. Email address: leeyh@sprc2.chonbuk.ac.kr

[1] R. G. Hennig, J. Chem. Phys. **40**, 2877 (1964); R. G. Hennig, Science **147**, 733 (1965).
[2] E. L. Evans *et al.*, Science **171**, 174 (1971).
[3] R. T. Yang and C. Wong, Science **214**, 437 (1981).
[4] H. Chang and A. J. Bard, J. Am. Chem. Soc. **112**, 4598 (1990).
[5] X. Chu and L. D. Schmidt, Carbon **29**, 1251 (1991); X. Chu and L. D. Schmidt, Surf. Sci. **268**, 325 (1992).
[6] A. Tracz *et al.*, Langmuir **9**, 3033 (1993); A. Tracz *et al.*, Langmuir **11**, 2840 (1995).
[7] D. E. Rosner and H. D. Allendorf, in *Heterogeneous Kinetics of Elevated Temperatures*, edited by G. R. Belton and W. L. Worrel (Plenum, New York, 1970).
[8] Y. W. Yang and J. Hrbek, J. Phys. Chem. **99**, 3229 (1995).
[9] F. Atamny *et al.*, J. Phys. Chem. **96**, 4522 (1992).
[10] J. R. Hahn *et al.*, Phys. Rev. B **53**, R1725 (1996).
[11] J. R. Hahn, Ph.D. thesis, Pohang University of Science and Technology, Korea, 1998.
[12] DMOL3 is a registered software product of Molecular Simulations Inc.; B. Delley, J. Chem. Phys. **92**, 508 (1990).
[13] J. P. Perdew and Y. Wang, Phys. Rev. B **45**, 13 244 (1992).
[14] A. D. Becke, J. Chem. Phys. **88**, 2547 (1988).
[15] The binding energy of graphite (-8.5 eV/atom) is overestimated, as expected from LDA calculations. However, we expect the energy difference of different structures to be of a small error. We have tested the size dependence by using a larger size (6×6) cell. Changes in energies were within 0.1 eV/atom. We have used Fermi-level smearing of 0.1 a.u. for fast convergence in the geometry optimization. The absolute binding energy became weaker, but changes in relative energies were negligible.
[16] We searched for an O_2 precursor state that may exist when edges of vacancies on two adjacent layers are close to each other. However, O_2 dissociates again and forms top and bridge sites on either layer, similar to that on a single layer.
[17] D. R. Olander *et al.*, J. Chem. Phys. **57**, 408 (1972).